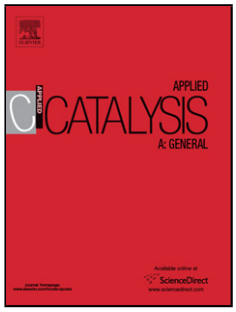

Title: Amine-functionalized hyper-crosslinked polyphenanthrene as a metal-free catalyst for the synthesis of 2-amino-tetrahydro-4*H*-chromene and pyran derivatives

Authors: Reddi Mohan Naidu Kalla, Anuraj Varyambath, Mi Ri Kim, Il Kim

PII: S0926-860X(17)30108-4
DOI: http://dx.doi.org/doi:10.1016/j.apcata.2017.03.009
Reference: APCATA 16168

To appear in: *Applied Catalysis A: General*

Received date: 21-12-2016
Revised date: 1-3-2017
Accepted date: 9-3-2017

Please cite this article as: Reddi Mohan Naidu Kalla, Anuraj Varyambath, Mi Ri Kim, Il Kim, Amine-functionalized hyper-crosslinked polyphenanthrene as a metal-free catalyst for the synthesis of 2-amino-tetrahydro-4H-chromene and pyran derivatives, Applied Catalysis A, General http://dx.doi.org/10.1016/j.apcata.2017.03.009

Amine-functionalized hyper-crosslinked polyphenanthrene as a metal-free catalyst for the synthesis of 2-amino-tetrahydro-4*H*-chromene and pyran derivatives

Reddi Mohan Naidu Kalla, Anuraj Varyambath, Mi Ri Kim, and Il Kim*

BK21 PLUS Centre for Advanced Chemical Technology, Department of Polymer science and Engineering, Pusan National University, Busan, Republic of Korea.

***Corresponding author**

E-mail: ilkim@pusan.ac.kr

Graphical abstract

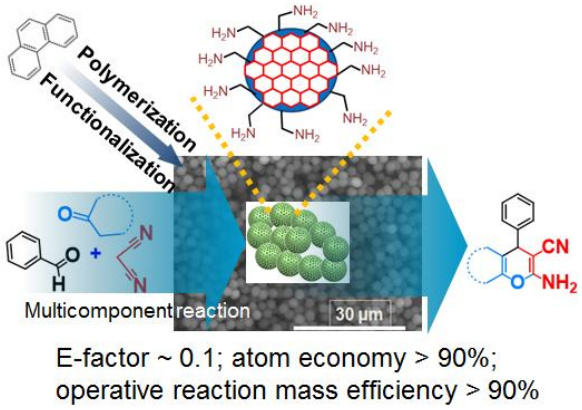

Highlights

- ▸Supported organo base-catalyzed syntheses of chromenes and pyrans are introduced.

- ▸The reactions are eco-friendly, economically viable and versatile.
- ▸ The catalyst is reusable without losing its catalytic activity.

ABSTRACT: The hyper-crosslinked microporous polyphenanthrene spheres were fabricated simply by the polymerization of phenanthrene using bromomethyl methyl ether as a bridging agent in the absence of any templates. The organic spheres were subjected to amine-functionalizing on the periphery of them using unreacted bromomethyl groups. The amine-functionalized microporous polyphenthrene could be employed as a highly effective and stable solid basic catalyst for the syntheses of functionalized 2-amino-tetrahydro-4*H*-chromene and pyran derivatives. The significant features of these reactions are high product yields, environmental benignity, short reaction time, broad substrate scope, and non-requirement of toxic solvents. Furthermore, the catalyst can be reused up to four times without significant loss of activity.

Keywords: Base catalyst, Carbon sphere, Chromenes, Multi-component reactions, Pyrans, Supported catalyst.

1. Introduction

The microporous organic polymers (MOPs) with pores smaller than 2 nm have attracted considerable interest due to their potential applications in the areas of catalysis, gas storage, molecular separation, conductivity [1]. Various synthetic methodologies and further chemical modifications of MOPs are widely reported [2–4].Over the past few years, researchers have developed variety of MOPs that are composed of non-metallic elements such as C, H, O, N, and B, including polymers of intrinsic micro porosity [5], covalent organic frameworks [6], and

conjugated microporous polymers [7]. The monomers used for these materials usually carry ethynyl [8] or stereo-controlled structures [9], which require tedious synthesis and purification using expensive catalysts [10].

Hyper-crosslinked microporous organic polymers (HMOPs) are a subclass of porous polymers, which are mainly synthesized by a hyper-crosslinking of small organic molecules by Friedel−Crafts alkylation reaction with external cross linker [11,12]. For example, the HMOPs were prepared by the post-cross linking reaction of styrene or styrene-divinylbenzene polymer in solution or a highly swollen state Davankov resin [13]. However, this method yielded HMOPs with humdrum polymeric matrices of non-uniform pores, and needed fussy synthesis processes. Recently we have fabricated highly uniform HOMPs based on a simple Friedel-Crafts alkylation of aromatic hydrocarbons including naphthalene, anthracene, phenanthrene, pyrene and coronene, showing good performance as super capacitor materials [14]. Since the resultant HMOPs are chemically and thermally stable and bear halogen functional groups on the surface, they can be easily functionalized without losing their morphology.

Currently, functionalized polymer materials with high surface area are receiving significant interest in the fields of adsorption, catalysis, sensor technology, and chromatography [7b,15]. Functionalization of the polymer material peripheral surface provides an efficient barrier against oxidation and acid erosion. Various methods have been developed for functionalization including post-modification, copolymerization of skeleton molecules with functional groups, and self-polymerization of functional organic groups. These supports have advantages like high chemical and hydrothermal stabilities and easy tailoring of active sites [16]. For the functionalization on the surface of porous polymers Xiao et al. employed sulfonic acid functionalized porous polymer for esterifications and Friedel–Crafts acylation reactions [17], Copper et al. reported the post-

modification of amine functionalized conjugated microporus polymers for gas sorption [18], and Wang et al. studied organic polymers functionalized with Tröger's base and 4-(N,N-dimethylamino)pyridine as the heterogeneous organocatalyst, showing reasonable catalytic activity in the addition reaction of diethyl zinc to 4-chlorobenzaldehyde and the acylation of alcohols and phenols [19,20].

Recent reports on ethylenediamine (EDA)–functionalized grapheneoxide (GO) indicate good catalytic activity in hydrolysis, Knoevenagelcondensation (KC) [21,22], and Henry-Michael reactions [23]. In view of the above, herein we report for the first time the synthesis of a HMOP featuring EDA covalently bonded to the bromomethylated HMOPs via condensation reaction. The unreacted bromomethyl groups can further chemically modified with EDA (Fig. 1). Phenanthrene (Ph) was chosen as starting material in this study due to its low cost and ready availability. The resultant polyphenanthrene PPh@EDA samples showed good catalytic activity for the preparation of biologically potent functionalized 2-amino-tetrahydro-4*H*-chromene and pyran derivatives. EDA is a liner with two nitrogen atoms, and its functionalization by various reduction condensation reactions, together with ionic liquids and various acids, is prominent in catalysis and other applications [24].

Recently, various important biologically potent heterocyclic compounds have been synthesized under solvent-free conditions via multicomponent reactions (MCRs) [25]. MCRs are an elegant and powerful tool for organic synthesis as compared to multistep reactions, due to the one-pot formation of several new bonds (e.g., C–C, C–N, C–O, and C–S). The advantages of MCRs are high atom economy, avoidance of time-consuming protection and deprotection processes,

simplicity, and shorter reaction time. Therefore, academic and industrial research is mainly focused on various organic transformations utilizing one-pot MCRs.

Derivatives of 2-amino-tetrahydro-4*H*-chromene and pyran, representing the main structural unit of most oxygen-containing heterocyclic compounds, are formed through one-pot Knoevenagel-Michael cyclocondensation. In addition, many natural products exhibiting anti-tumor/cancer, antiviral, antibacterial, antifungal, anticoagulant, antileishmanial, antiallergenic, and diuretic activities contain chromene moieties [26]. For example, 2-amino-tetrahydro-4*H*-chromene derivatives **A**, **B**, and **C** are valuable compounds (Fig. 2) [27–30]. Compound **A** is a tumor antagonist that exhibits binding activity for the surface pocket of cancer-implicated Bcl-2 proteins and induces apoptosis in follicular lymphoma-B and leukemia HL-60 cells. Compound **B** is an inhibitor of the insulin-regulated amino peptidase (IRAP), enhancing memory and learning functions, while compound **C** and its derivatives are antibacterial agents.

Furthermore, these compounds are used in other applications, such as fluorescence markers [31], laser dyes [32], pigments [33], optical brighteners [34], cosmetics, and pH-sensitive fluorescent materials for the visualization of biomolecules [35] and biodegradable agrochemicals [36]. Owing to their important properties, various methods for preparing 2-amino-tetrahydro-4*H*-chromenes and pyrans have been developed, e.g., methods utilizing microwaves [37], PPA-SiO_2 [38], meglumine [39], MgO [40], triethylamine [41], urea [42], ionic liquids [43], and Fe_3O_4 nanoparticles (NPs) supported by multi-walled carbon nanotubes [44]. However, the majority of these methods suffer from certain drawbacks such as long reaction times, expensive non-reusable catalysts, toxic solvents, and tedious work-up procedures. Hence, a search for more broad, feasible, clean, efficient, and high-yielding routes to this class of *O*-heterocycles remains a valid exercise.

The important goals of green chemistry include the avoidance of organic solvents, toxic reagents, and the reduction of costs associated with organic synthesis. In view of these goals and our sustained interest in the development of efficient, economical, and novel methodologies [45–47], we herein report the use of easily accessible PPh@EDA as an environmentally benign and recyclable solid basic catalyst for high-yielding and solvent-free synthesis of chromenes and pyrans (Scheme 1).

2. Experimental

2.1. Materials and instrumentation

Aromatic hydrocarbons such as Ph (98%, Sigma-Aldrich), and Co (>95%, TCI), Bromomethyl methyl ether (BMME, >95%, TCI), various substituted aldehydes, (Sigma-Aldrich Co.) malononitrile (Fisher Scientific UK Ltd), cyclicketones and acyclic ketones (TCI), anhydrous zinc bromide ($ZnBr_2$, 98%, Acros), were used as received. All experiments were performed under solvent-free conditions. Pre-coated silica gel plates (Merck Chemicals) were developed with iodine, and were used for analytical thin-layer chromatography (TLC). Melting points were uncorrected and determined using a digital Stuart SMP3 apparatus (Bibby Scientific Limited, Staffordshire, UK). ^{1}H NMR (400 MHz), and ^{13}C NMR (100 MHz), spectra were recorded using a Varian INOVA 400 NMR spectrometer at room temperature. Chemical shift values are quoted relative to Me_4Si. Data are presented as follows: chemical shift (ppm), multiplicity (s= singlet, d = doublet, dd = doublet of doublets, t = triplet, m = multiplet), and coupling constant *J*(Hz). Solid ^{13}C NMR spectra were obtained on a Bruker Avance 500 NMR spectrometer. Fourier-transform (FT) IR spectra were recorded at r.t. using a Shimadzu IR Prestige 21 spectrometer. The spectra were obtained, using KBr disks, in the range 4500–500 cm^{-1}. The XRD analysis was performed by using an automatic Philips powder diffractometer with nickel-filtered Cu Kα radiation. The

diffraction pattern was collected in the 2 range of 0-80ºin steps of 0.02º and counting times of 2 s step^{-1}. The microstructures of the samples were investigated using an S-3000 scanning electron microscope (SEM; Hitachi, Japan) and thermo gravimetric analysis measured by TGA N-1000 (Scinco, Seoul, and Republic of Korea).X-ray photoelectron spectroscopy (XPS) analysis was performed in a Theta Probe AR-XPS system with a monochromatic Al Kα X-ray source (1486.6 eV). The Brunauer-Emmett-Teller (BET) and the Density-Functional-Theory (DFT) methods (Nova 3200e system, Quantachrome Instrument, USA) were used to investigate the BET specific surface area and pore size distribution of the samples. Elemental analyses were obtained on GmbH elemental analyzer.

2.2. Synthesis of bromomethylatedpolyphenanthrene, PPh@CH_2Br.

Phenanthrene (1 g, 5.6 mmol)and anhydrous $ZnBr_2$ (1.3 g, 5.7 mmol) were dissolved in dichloroethane (80 mL)in a 100 mL flask, and bromomethyl methyl ether (BMME) (1.4 g, 11.2 mmol) was added to the solution under an atmosphere of nitrogen. The mixture was stirred for 18 h at 70 °C, and the resulting polymer was thoroughly washed with water and methanol. After extraction with methanol in a Soxhlet extractor for 24 h, the synthesized bromomethylatedpolyphenanthrene (PPh@CH_2Br) polymer was collected and dried overnight under vacuum at 110 °C. The addition of BMME introduced methylene crosslinking bridges between PPh rings, and the bromine content of the non-cross linked part (–CH_2Br) was determined by calorimetrically [48].

2.3.Functionalization of PPh@CH_2Br with EDA.

PPh@CH_2Br (0.6 g) was dissolved in CH_2Cl_2 (15 mL) in a 25 mL flask and EDA (1.8 mL) was added slowly at r.t. The mixture was stirred for 12 h at r.t. The resulting EDA–functionalized

polymer was centrifuged, washed with CH_2Cl_2 (10 mL), and dried at 80 °C for 4h. The EDA functionalized PPh@EDA was designated as PPh@EDA–0.2, PPh@EDA–0.4, and PPh@EDA–0.6, where the 0.2, 0.4, and 0.6 represent the amount (mL) of EDA used during the preparation of the PPh@EDA samples.

*2.4. General procedure for the preparation of 2-amino-tetrahydro-4H-chromene and pyran derivatives **1–42**.*

p–methoxybenzaldehyde 1{11} (1 mmol), MN 2{1} (1 mmol), dimedone 3{1}(1 mmol), and PPh@EDA (10 mg) were mixed at r.t. under solvent-free conditions with stirring. The reaction progress was monitored by TLC (hexane:EA = 6:4). When the reaction was complete, EA (8 mL) was added, and the reaction mixture was centrifuged for 30 min at 6000 rpm. The solvent was decanted and concentrated using a rotary evaporator. The crude product was purified by recrystallization from EtOH (10 mL). This procedure was used for all title compounds. In the re-usability tests, PPh@EDA was washed with EA (2 × 8 mL) and dried under vacuum at 80 °C for 1h. Detailed spectral data for all the compounds, ^{1}H and ^{13}C NMR are given in the Supporting Information (SI).

3. Results and Discussion

3.1. Characterization of PPh@EDA.

To assess the extent of EDA incorporation onto PPh bearing bromide groups on the periphery (PPh@CH_2Br), Fourier transform infrared (FT-IR) spectra of individual PPh@CH_2Br and PPh@EDA samples were recorded (Fig. 3(A)). The characteristic peaks of PPh@CH_2Br are due to the C–H wagging vibration at 1190 cm^{-1} and the C–Br stretching vibration at 750 cm^{-1} of the CH_2Br moiety. For PPh@EDA, the broad peak at 3441 cm^{-1} corresponds to the both –NH and –NH_2 group, and the new peak at 1344 cm^{-1} is attributed to the C–N bond [21].In addition,

depending on the amount of the amine, the peak intensities of –NH, $–NH_2$ and C–Br changes due to the reaction between amine and uncroslinked bromine. The C–Br stretching vibrations nearly disappeared, indicating the occurrence of amination to produce PPh@EDA. In addition the C–N bond of PPh@EDA is clearly shown in solid state ^{13}C NMR spectrum Fig. S1 in the SI.

X-ray powder diffraction (XRD) spectra of PPh@CH_2Br and PPh@EDA samples are shown in Fig. 3(B). Generally, carbon materials exhibit a (002) reflection peak at 2θ=26.6°[49].The shift of the latter to lower angles (2θ=23.3°) indicates C–N bond formation as a result of EDA functionalization of PPh [22].The thermal stabilities of PPh@CH_2Br and PPh@EDA were measured by thermo gravimetric analysis (TGA, Fig. 3(C)). The weight loss in the range of 300–370 °C is due to the pyrolysis of labile oxygen-containing functional groups, producing CO and CO_2. Furthermore, the thermal stability threshold of PPh@EDA is below 300°C, which is lower than that of PPh@CH_2Br due to earlier degradation of ethylene moieties. The surface morphology of PPh@CH_2Br and PPh@EDA was investigated using scanning electron microscopy (SEM). The observed microsphere sizes (30 μm) were uniform (Fig. 3(D)), attributed to the uniform bromomethylation layer on the surface of aromatic hydrocarbons during polymerization. The morphology of PPh@EDA was similar to that of PPh@CH_2Br (Fig. 3(D)), indicating no change of surface morphology in the reaction of the polymer with EDA.

The textured morphology of the HMOPs sample was further investigated by nitrogen adsorption-desorption. In all cases, the nitrogen absorption-desorption isotherms were type IV curves (Fig. 3(E)). The BET surface area of PPh@EDA-0.6and PPh@EDA-0.4was estimated as 552 m^2/g and 556 m^2/g indicating good porosity of the PPh@EDA samples. The total pore volume of PPh@EDA was measured to be 0.38 cm^3g^{-1}. In addition, as shown DFT calculations derived from the pore size distribution showed that peak value observed at 9.2 A^0 and 9.6 A^0 for PPh@EDA-0.6 and

PPh@EDA-0.4. This suggests that the size of the micropores arises from spherical structures formed by regular crosslinking on surface of the polymer.

X-ray photoelectron spectroscopy (XPS) is a quantitative surface analysis technique, used to determine empirical formulae, elemental composition (at parts per thousand ranges), and the chemical and electronic states of the elements present in the sample. Fig. 4 shows the C1s, N1s, and O1s regions of the PPh@EDA XPS spectra. The C1s region shows three distinct carbon environments at 284.5, 284.7, and 284.9 eV, corresponding to sp^2 C, (C–C/C=C), and C–N functionalities, respectively [17]. Figure 4(D) clearly shows that the N1s spectra can be fitted by two curves with binding energies of 398.6 and 399.7 eV, assigned to –C–NH and CH_2–NH_2, respectively [50]. The presence of these two peaks indicates that the condensation of EDA with PPh@CH_2Br results in the formation of C–N bonds. Element analysis of PPh@EDA showed that the amounts of C, H and N are 85.98, 5.60 and 1.78 wt%, respectively.

3.2. PPh@EDA-catalyzed synthesis of functionalized 2-amino-tetrahydro-4H-chromenes and pyrans.

The characterizations above confirm the successful functionalization of EDA into the HMOP of PPh matrix and the importance of aromatic hydrocarbons are widespread components of many materials, such as petroleum and tars. Generally the aromatic hydrocarbons present in mixtures, occurring both naturally and as byproducts of fuel processing operations. Phenanthrene is a polycyclic aromatic hydrocarbon (PAH) compounds that consists of sp^2-hybridized carbon atoms, forming a uniform hexagon, similar to graphite. These PAHs, since they are assembled from aromatic rings in a periodic fashion, possess extraordinary and often unique electronic properties, and also it shows low bond gaps, will inspire research on solar cell devices, semiconductors,

molecular sensors, and UV stabilizer/absorbers. By using this material we study the catalytic activity for the synthesis of 2-amino-tetrahydro-4*H*-chromenes and pyrans through MCRs. It requires extensive reaction times, high temperatures, and high catalyst loading to promote the formation of the desired product. Reactions taking place under solvent-free (neat) conditions have attracted significant interest, since they are cost-effective, easy to handle, require simple workup procedures, and lead to high yields. Recently, we have synthesized various biologically potent organic compounds under solvent-free conditions [51–54]. One-pot three-component reactions of *p*-methoxy benzaldehyde, malononitrile (MN), and dimedone (1 mmol each) were first attempted using catalyst-free, acidic (Heterogeneous and Lewis acids) and basic (liquid and solid) catalysts at room temperature (r.t.) under solvent-free conditions. We found that the solid basic PPh@EDA catalyst was best suited for the formation of target 2-amino-tetrahydro-4*H*-chromenesin good yields, preventing the occurrence of Knoevenagel condensation (KC) (Scheme 2).

Initially, the reaction between *p*-methoxybenzaldehyde, MN, and dimedone was conducted in absence of catalyst at r.t. for 14 h under solvent-free conditions; however, no product was observed (Table 1, entry 1). Later, acidic catalysts such as $AlCl_3$, $FeCl_3$, $CuCl_2$,silicotungstic acid (STA), phospho sulfonic acid (PSA), and tungstosulfonic acid (TSA) were used at r.t. for 5h,furnishing yields below 50% and requiring tedious workup procedures (entries 2–7). Subsequently, basic catalysts containing primary, secondary and tertiary nature were employed. At first, the same reaction was conducted in presence of 4-ethylmorpholine as catalyst (3 mol %). After 1h, the reaction mixture contained both the KC and the targeted 2-amino-tetrahydro-4*H*-chromene products in a ratio of 0.5:1, estimated from the corresponding ^{1}H NMR spectrum (Fig. S3, SI). No

changes were observed when the reaction was continued for 8 h under the same conditions (entries 8–10).

Based on these results, we tried to find a suitable basic catalyst for the selective formation of 2-amino-tetrahydro-4*H*-chromenes and pyrans over the KC product. Various basic catalysts, such as triethylamine, ^{t}butylamine, tetramethylethylenediamine (TMEDA), pyrrolidine, piperidine, and diethylamine (DEA) furnished the desired 2-amino-tetrahydro-4*H*-chromenes and pyrans in excellent yields, without the formation of KC product (Table 1, entries 11–16). The Jeffamine polymers with three different molecular weights (230, 400, and 2000) bearing, □α,ω-amine groups provided the desired products with good yields without forming intermediates (entries 17–19); however, the reaction systems involving these polymers are homogeneous and it needs tedious protocols to purify and separate them after the reaction. We have also employed solid polymers containing primary amine, poly(ethylene glycol) methyl ether amine (MPEG2000–NH_2; MW=2000) and tertiary amine, poly(dimethyl amino ethyl methacrylate) (PDMAEMA) for the synthesis of targeted compounds. These two catalysts also show good activities (entries 20 and 21), but again the separation of these polymers is not easy.

The same reaction conducted in presence of resin such as Amberlite IRA–410 gives good yield but it takes long time for completion of the reaction (entries 22). In order to circumvent this problem, we have prepared microporus PPh@EDA as a solid basic catalyst and applied it for the selective formation of 2-amino-tetrahydro-4*H*-chromenes and pyrans. Initial trials to use PPh@CH_2Br for the reaction show only negligible catalytic activity. To increase the rate of the reaction and yield of the product, we substituted the bromine groups for EDA with various amount of amine (0.2, 0.4, and 0.6 mL). Comparing all the three PPh@EDA samples, PPh@EDA–0.6

showed the best catalytic activity for the targeted compounds (entries 26–31), indicating that the number of basic sites has a significant effect on the catalytic performance. The optimal molar loading of PPh@EDA was determined in a model reaction using 1.8, 3, 3.6, 4.8, 6, and 7.8 mol % of PPh@EDA under neat conditions, producing the target compound in 80, 82, 87, 91, 95, and 95% yield, respectively. The yields gradually increased with increasing catalyst loading up to 6 mol %, with no enhancement of the product yield observed at higher loadings (entries 26–31).

Subsequently, the reaction progress under solvent and solvent-free conditions (Table 2) was compared. The reaction preceded smoothly in both polar and non-polar solvents, such as ethanol, isopropanol, methanol, THF, CH_2Cl_2, $CHCl_3$, and 1,4-dioxane. Both solvent groups led to the effective formation of target compounds, but the reaction times required were long (entries 2–8).

The scope and limitations of this catalytic method were investigated using diverse aldehydes **1**{1−20}, alkylmalonates **2**{1, 2}, and cyclic ketones **3**{1,2}; acyclic ketoesters {3–5} were selected for library validation (Fig. 5). First, the reaction of *p*-methoxybenzaldehyde **1** {11}, MN **2** {1}, and dimedone **3**{1} was examined. As shown in Table 3, this MCR produced a good yield of the desired product in a short time. The nature of substrate and the position of functional groups in the aromatic ring of the aldehyde had a small effect on product yield and reaction time.

Aromatic aldehydes with electron-donating groups (OMe, OEt) in the para-position reacted faster and gave better yields compared to the ones with the above groups in the ortho-position, due to steric hindrance. The same effects were also observed for aldehydes with alkyl groups (Me or ^{i}Pr). While halogen-substituted aldehydes furnished good yields and fast reaction rates, those substituted at the 2-position reacted slower than the ones substituted at 3-and 4-positions. 2-chloro-6-fluorobenzaldehyde gave yields smaller than those of other halogen-substituted aldehydes, due

to the electro-negativity of the fluorine substituent. Reactions of aldehydes bearing a highly electron-withdrawing nitro group were relatively slow and furnished the products in low yields, due to the electron deficiency of the substrate. Furthermore, heterocyclic and aliphatic aldehydes also gave good yields and short reaction times. We found that the reaction with ethyl cyanoacetate was slower than that with MN, due to the lower reactivity of the former. Subsequently, activated compounds with enolizable C−H bonds, such as cyclohexane-1,3-dione, containing a reactive α-methylene group, were also evaluated. Furthermore, the reaction was extended to compounds containing acyclic ketoester moieties, such as methylacetoacetate, ethylacetoacetate, and ^{t}butylacetate, the reactions of which proceeded smoothly, with total avoidance of KC (Table 3, entries 26–41).

In addition, the merits of microporus PPh@EDA were compared with those of other reported amine containing various porous and nonporous catalysts for the synthesis of 2-amino-4*H*-chromenes and pyrans (Table 4). Aghayanet al. [55] developed for the synthesis of tetrahydro-chromenes in presence of mesoporous amino-functionalized MCM–41 catalyst that is active only at high temperatures, leading to the formation of by products. Recently Morsali [56] reported the synthesis of tetrahydro−chromenes by using amine−functionalized metal−organic framework (MOF–NH_2) that is active in organic solvents and needs long reaction time (4 h) to complete the reaction at reflux condition. Liao et al. [57] also reported the use of amino–appended β–cyclodextrins supramolecular catalyst (β–CD–NH_2) for the preparation of 2-amino-4*H*-chromenes needing longer reaction time than PPh@EDA. Siddiqui et al.[58] used chitosan as a catalyst for the synthesis of 2-amino-4*H*-pyrans, requiring 1.5 h to achieve 89% yield. Comparing to above-mentioned catalysts, the PPh@EDA has obvious advantages for the synthesis of 2-amino-4*H*-

chromenes and pyrans in that it does not require harsh reaction conditions, solvents and laborious work-up procedures and that it is recyclable. Such an attractive features of PPh@EDA are related with the hyper-cross-linked micropore structure of it. The presence of interconnected micropores may result in (i) a beneficial mass transfer from side to side; (ii) a large surface area available for interaction of the molecules with the active sites [59,60]. These micropores present a good platform for the catalysis to carry on in a particular pathway leading to the desired products by virtue of its decreased retention times.

Finally, the recyclability of PPh@EDA was examined for the preparation of functionalized 2-amino-tetrahydro-4*H*-chromene **4**{11,1,1}. PPh@EDA was simply recovered by adding ethyl acetate (EA) to the reaction mixture. The insoluble catalyst was separated by centrifugation, washed twice with EA (2 × 8 mL), and dried under vacuum at 60 °C, showing good reusability for up to 4 cycles the catalytic activity was slightly decreased due to the recovery percentage of the catalyst might be loss during recovery (Fig. 6), and also the recycled catalyst was characterized by using FT-IR, TGA and SEM is similar to that of fresh catalyst (Fig. S2, SI).

All synthesized compounds were identified by FT-IR, ^{1}H, and ^{13}C NMR spectroscopies. The IR spectra of compounds **1–42** showed the expected absorption bands at 3425–3119, 2346–2356, and 1750–1650 cm^{-1}, attributed to NH_2, CN, and C=O stretching vibrations, respectively [39]. In ^{1}H NMR spectra, the Ar–CH proton signal appeared as a singlet at 5.16–3.38 ppm, and the NH_2 signal appeared as a broad singlet at 4.75–4.42 ppm. The remaining proton signals were in agreement with the ones previously reported. In ^{13}C NMR spectra, the Ar–CH carbon signal at 40.4 ppm confirmed the formation of target compounds.

A plausible reaction mechanism for the formation of functionalized 2-amino-tetrahydro-4*H*-chromenes and pyrans in the presence of PPh@EDA is shown in Scheme 3. Initially, the aldehyde

carbonyl group reacts with malononitrile to form the KC product. Subsequently, the enol form of active methylene compounds undergoes Michael addition to the KC product and forms the desired 2-amino-tetrahydro-4*H*-chromenes after cyclization.

4. Conclusions

We have reported active, stable and recyclable micropores PPh@EDA systems highly effective solid base catalysts for the synthesis of 2-amino-tetrahydro-4*H*-chromenes and pyrans. This catalyst is applicable for broad substrate scope and the reactions involving PPh@EDA catalyst are characterized by operational simplicity, good yields, mild reaction conditions, short reaction times, easy recovery and recycling of catalyst, chromatography–free purification, and no use of hazardous and expensive organic solvents. Thus, **4**{11,1,1} compound was obtained at 95% yield by reacting *p*-methoxybenzaldehyde **1**{11} (1 mmol), MN **2**{1} (1 mmol), and dimedone **3**{1}(1 mmol) at r.t. under solvent-free conditions by using PPh@EDA (10 mg) as a catalyst in an hour. In addition the catalyst was recyclable 4 times without losing its activity. Evidently PPh@EDA is an environmentally friendly and commercially tangible catalyst for the preparation of diverse libraries of 2-amino-tetrahydro-4*H*-chromene and pyran derivatives.

Justification

We summarize the contribution of this research as follows.

i) A diversity of 2-amino-tetrahydro-4*H*-chromene and pyrans were synthesized with high yields in a short time by using amine-functionalized polyphenanthrene spheres as a catalyst for the first time. All compounds were fully characterized by IR, ^{1}H and ^{13}C NMR.

ii) An efficient and green method was employed for the synthesis of these derivatives.

iii) The amine-functionalized polyphenanthrene catalyst was a found to be more suitable for the synthesis of targeted compounds compared with the reported methods.

Acknowledgements

This work was supported by the Basic Science Research Program through the National Research Foundation of Korea (2015R1D1A1A09057372). The authors also thank the BK21 PLUS Program for partial financial support.

References

[1] R. Dawson, A.I. Cooper, D.J. Adams, Prog. Polym. Sci. 37 (2012) 530–563.

[2] S. Xu, Y. Luo, B. Tan, Macromol. Rapid Commun. 34 (2013) 471–484.

[3] G. Jonathan, M.J.F. Jean, S. Frantisek, Small, 5 (2009) 1098–111.

[4] J. Jiang, A.I. Cooper, M. Schroder, *Microporous Organic Polymers: Design, Synthesis, and Function. Functional Metal-Organic Frameworks: Gas Storage, Separation and Catalysis*; Springer, 2010.

[5] G. Cheng, B. Bonillo, R.S. Sprick, D.J. Adams, T. Hasell, A.I. Cooper,Adv. Funct. Mater. 24 (2014) 5219–5224.

[6] Q. Fang, Z. Zhuang, S. Gu, R.B. Kaspar, J. Zheng, J. Wang, S. Qiu, Y.Yan, Nat. Commun.5 (2014) 4503.

[7] R. Dawson, A. Laybourn, Y.Z. Khimyak, D.J. Adams, A.I. Cooper, Macromolecules, 43 (2010) 8524–8530.

[8] S. Yuan, B. Dorney, D. White, S. Kirklin, P. Zapol, L. Yu, D. Liu, Chem. Commun.46 (2010) 4547–4549.

[9] X.D. Zhuang, F. Zhang, D.Q. Wu, N. Forler, H.W. Liang, M. Wagner, D. Gehrig, M.R. Hansen, F. Laquai, X.L. Feng, Angew. Chem., Int. Ed. 52 (2013) 9668–9672.

[10] B. Li, Z. Guan, W. Wang, X. Yang, J. Hu, B. Tan, T. Li,Adv. Mater.24 (2012) 3390–3395.

[11] P. Samanta, P. Chandra, S.K. Ghosh, Beilstein J. Org. Chem.12 (2016) 1981–1986.

[12] B. Li, R. Gong, W. Wang, X. Huang, W. Zhang, H. Li, C. Hu, B. Tan,Macromolecules,44 (2011) 2410–2414.

[13] M.P. Tsyurupa, V.A. Davankov, React. Funct. Polym.66 (2006) 768–779.

[14] X. Huang, S. Kim, M.S. Heo, J.E. Kim, H. Suh, I. Kim, Langmuir, 29 (2013) 12266–12274.

[15] K.E. Maly, J. Mater. Chem.19 (2009) 1781–1787.

[16] Q. Sun, Z. Dai, X. Meng, F.-S. Xiao, Chem. Soc. Rev.44 (2015) 6018–6034.

[17] F. Liu, X. Meng, Y. Zhang, L. Ren, F. Nawaz, F.-S.Xiao, J. Catal.271 (2010) 52–58.

[18] S. Jiang, J. Bacsa, X. Wu, J.T.A. Jones, R. Dawson, A. Trewin, D.J. Adams, A.I. Cooper, Chem. Commun. 47 (2011) 8919–8921.

[19] X. Du, Y. Sun, B. Tan, Q. Teng, X. Yao, C. Su, W. Wang, Chem. Commun.46 (2010) 970–972.

[20] Y. Zhang, Y. Zhang, Y.L. Sun, X. Du, J.Y. Shi, W.D. Wang, W. Wang, Chem. Eur. J.18 (2012) 6328–6334.

[21] F. Zhang, H. Jiang, X. Li, X. Wu, H. Li. ACS Catal.4 (2014) 394–401.

[22] B. Xue, J. Zhu, N. Liu, Y. Li, Catal .Commun.64 (2015) 105–109.

[23] F. Zhang, H. Jiang, X. Wu, Z. Mao, H. Li. ACS Appl. Mater. Interfaces.7 (2015) 1669–1677.

[24] N.H. Kim, T. Kuil, J.H. Lee, J. Mater. Chem.A1 (2013) 1349–1358.

[25] R.V.A. Orru, M. de Greef, Synthesis, 10 (2003) 1471–1499.

[26] L. Bonsignore, G. Loy, D. Secci, A. Calignano, Eur. J. Med. Chem.28 (1993) 517–520.

[27] M.N. Erichsen, T.H.V. Huynh, B. Abrahamsen, J.F. Bastlund, C. Bundgaard, O. Monrad, A.B. Jensen, C.W. Nielsen, K. Frydenvang, A.A. Jensen, L. Bunch, J. Med. Chem.53 (2010) 7180−7191.

[28] W. Kemnitzer, J. Drewe, S. Jiang, H. Zhang, C.C. Grundy, D. Labreque, M. Bubenick, G. Attardo, R. Denis, S. Lamothe, H. Gourdeau, B. Tseng, S. Kasibhatla, S.X. Cai, J. Med. Chem.51 (2008) 417−423.

[29] M. Mahmoodi, A. Aliabadi, S. Emami, M. Safavi, S. Rajabalian, A.M. Mohagheghi, A. Khoshzaban, A.S. Kermani, N. Lamei, A. Shafiee, A. Foroumadi, Arch. Pharm. Chem. Life Sci.343 (2010) 411−416.

[30] D. Kumar, V.B. Reddy, S. Sharad, U. Dube, S. Kapur, Eur. J. Med.Chem.44 (2009) 3805−3809.

[31] E.R. Bissell, A.R. Mitchell, R.E. Smith, J. Org. Chem.45 (1980) 2283−2287.

[32] G.A. Reynolds, K.H. Drexhage, Opt. Commun.13 (1975) 222−225.

[33] G.P. Ellis, "*Chromenes, Chromanones, and Chromones*," in The Chemistry of Heterocyclic Compounds Chromenes, A. Weissberger andE.C. Taylor, Eds., Wiley, NY, USA, 1977.

[34] H. Zollinger, *Color Chemistry: Syntheses, Properties, and Applications of Organic Dyes and Pigments*, VHCA, Zurikh, Switzerland, 3rd edn, 2003.

[35] C.G. Knight, T.J. Stephens, J.Bio.Chem.258 (1989) 683−687.

[36] E.A.A. Hafez, M.H. Elnagdi, A.G.A. Elagamey, F.M.A.A. El-Taweel, Heterocycles, 26 (1987) 903−907.

[37] S. Santra, M. Rahman, A. Roy, A. Majee, A. Hajra, Org. Chem. Int.2014, 1−8.

[38] A. Davoodnia, S. Allameh, S. Fazli, N. Tavakoli-Hoseini, Chem. Pap.65 (2011) 714−720.

[39] R.-Y. Guo, Z.-M. An, L.-P. Mo, ACS Comb. Sci.15 (2013) 557−563.

[40] M. Seifi, H. Sheibani, Catal. Lett.126 (2008) 275−279.

[41] M.H. Elnagdi, R.M. Abdel-Motaleb, M. Mustafa, M.F. Zayed, E.M. Kamel, J. Heterocycl. Chem.24 (1987) 1677−1681.

[42] G. Brahmachari, B. Banerjee, ACS Sustainable Chem. Eng.2 (2014) 411−422.

[43] Y. Peng, G. Song, Catal .Commun.8 (2007) 111−114.

[44] A. Fallah-Shojaei, K. Tabatabaeian, F. Shirini, S.Z. Hejazi, RSC Adv. 4 (2014) 9509−9516.

[45] R.M.N. Kalla, H. Park, H.R. Lee, H. Such, I. Kim, ACS Comb. Sci.17 (2015) 691−697.

[46] R.M.N. Kalla, S.J. Byeon, M.S. Heo, I. Kim, Tetrahedron, 69 (2013) 10544−10551.

[47] R.M.N. Kalla, V.J. Johnson, H. Park, I. Kim, Cat. Commun.57 (2014) 55–59.

[48] B. Niyazi, K. Bunyamin, Eur. Polym. J. 43 (2007) 4719–4725.

[49] R. Bissessur, P.K.Y. Liu, S.F. Scully, Synth. Met.156 (2006) 1023–1027.

[50] T. Ramanathan, F.T. Fisher, R.S. Ruoff, L.C. Brinson, Chem. Mater. 17 (2005) 1290–1295.

[51] K.R.M. Naidu, S.I. Khalivulla, S. Rasheed, S. Fakurazi, P. Arulselvan, O. Lasekan, F. Abas, Int. J. Mol. Sci.14 (2013) 1843–1853.

[52] K.R.M. Naidu, B.S. Krishna, M A. Kumar, P. Arulselvan, S.I. Khalivulla, O. Lasekan, Molecules, 17 (2012) 7543–7555.

[53] R.M.N. Kalla, M.R. Kim, I. Kim, Tetrahedron Lett.56 (2015) 717–720.

[54] R.M.N. Kalla, M.R. Kim, Y.N. Kim, I. Kim, New J. Chem.40 (2016) 687–693.

[55] M. Mirza-Aghayan, S. Nazmdeh, R. Boukherroub, M. Rahimifard, A.A. Tarlani, M. Abolghasemi-Malakshah, Synth.Commun.43 (2013) 1499–1507.

[56] V. Safarifard, S. Beheshti, A. Morsali, Cryst. Eng.Commun. 17 (2015) 1680–1685.

[57] Y. Ren, B. Yang, X. Liao, Catal. Sci. Technol.6 (2016) 4283–4293.

[58] P.R. Rahila, I. Afshan S. Hozeyfa R. Siddiqui, Chemistryselect, 1 (2016) 1300–1304.

[59] V. Meynen, P. Cool, E.F. Vansant, Microporous Mesoporous Mater.104 (2007) 26–38.

[60] S. van Donk, A.H. Janssen, J.H. Bitter, K.P. de Jong, Catal. Rev. - Sci. Eng.45 (2003) 297–319.

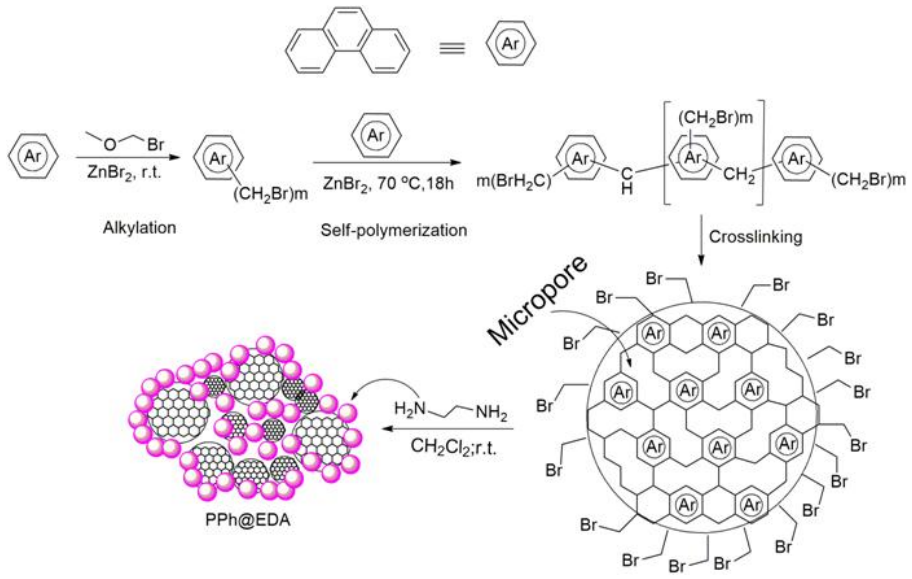

Fig. 1. Schematic synthesis of hyper-crosslinked polyaromatic spheres and ethylenediamine-functionalized polymer spheres (PPh@EDA).

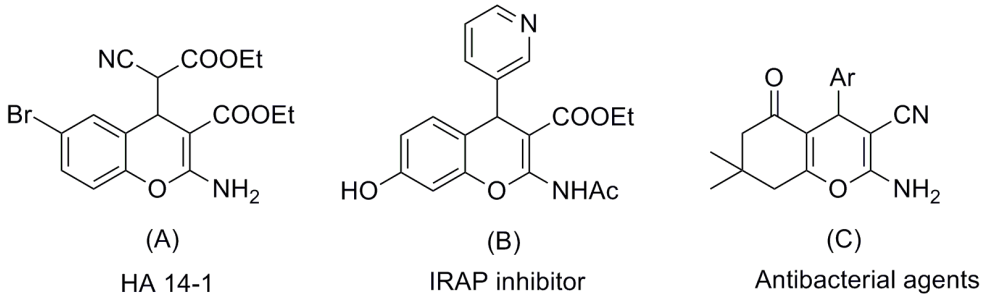

Fig. 2. Examples of representative 2-amino-tetrahydro-4*H*-chromene derivatives HA 14-1(A), IRPA inhibitor (B), and Antibacterial Agents (C).

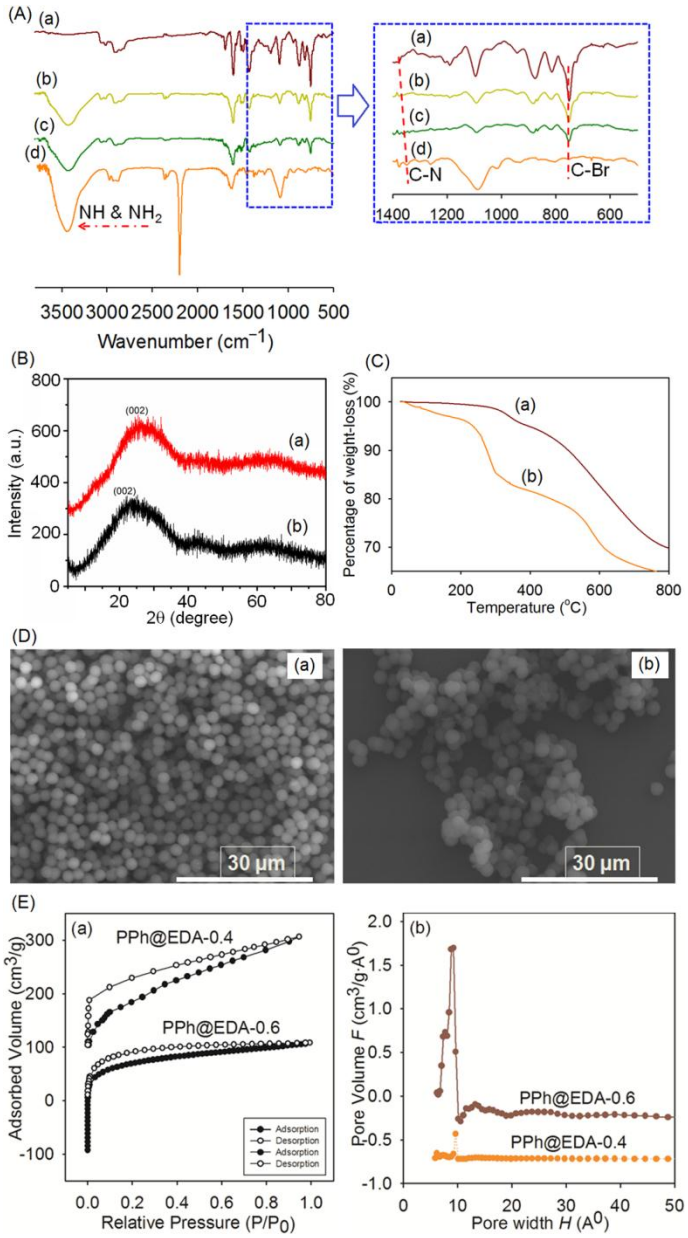

Fig. 3. (A) FT-IR spectra of PPh@CH_2Br (a), PPh@EDA–0.2 (mL) (b), PPh@EDA–0.4 (mL) (c), and PPh@EDA–0.6 (mL) (d); (B) XRD patterns of PPh@CH_2Br (a) and PPh@EDA (b); (C) TGA thermograms of PPh@CH_2Br (a) and PPh@EDA (b); SEM images of PPh@CH_2Br (a) and PPh@EDA (b); and (E) nitrogen adsorption and desorption isotherms (a) and pore size distribution (b) of PPh@EDA.

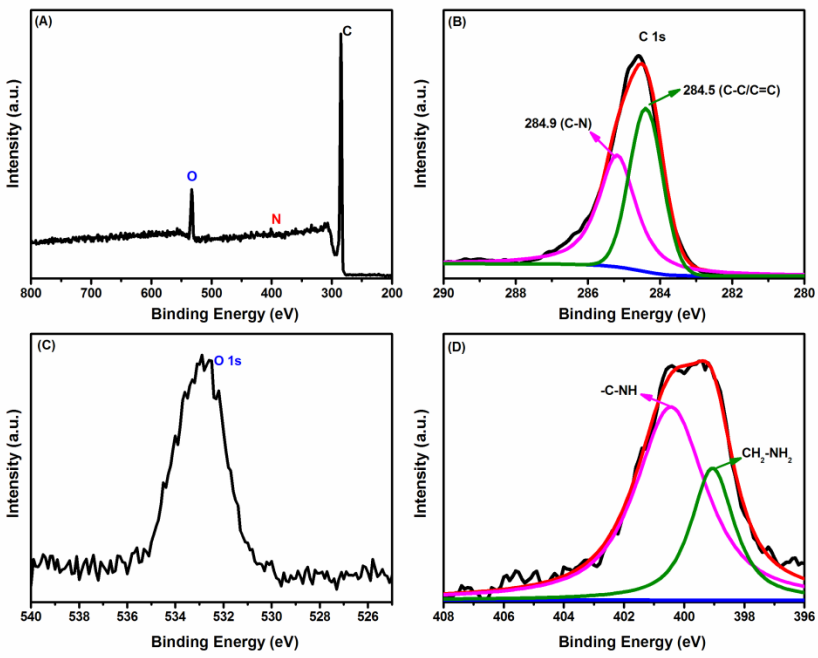

Fig. 4. XPS curves: full spectrum of PPh@EDA (A), with corresponding C1s (B), O1s (C), and N1s (D) regions.

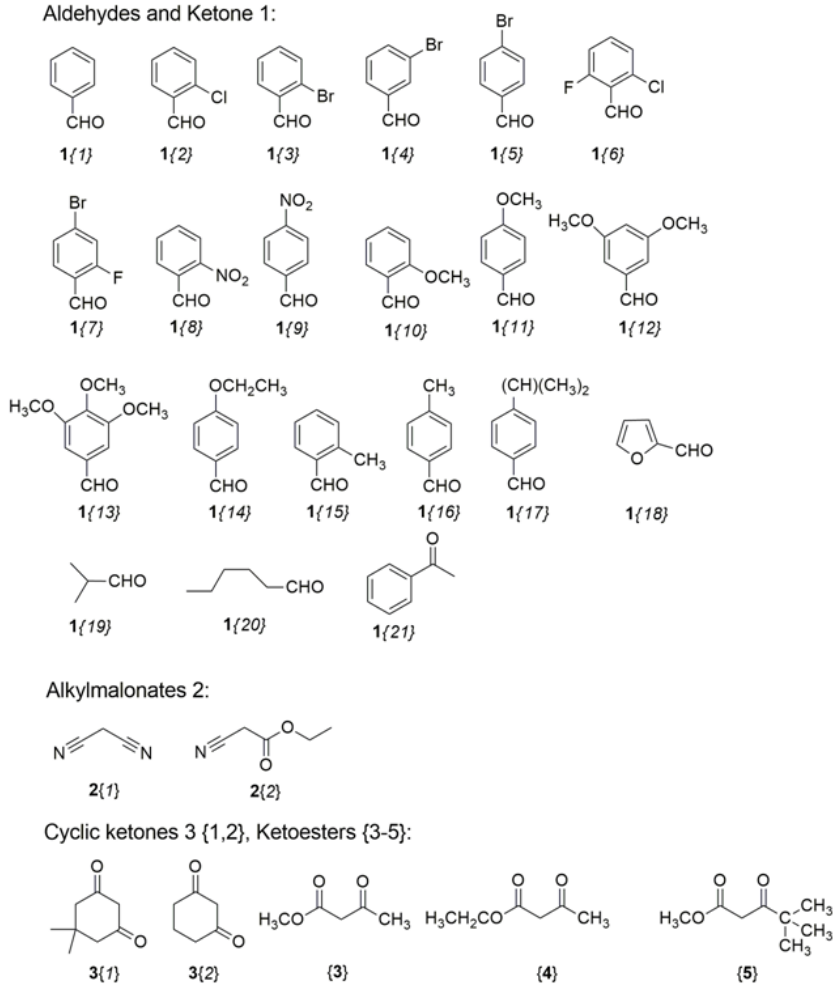

Fig. 5. Reagents used to study the reaction scope.

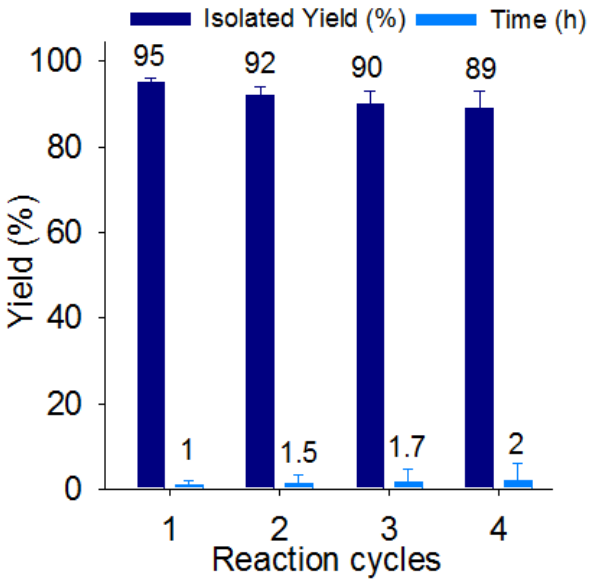

Fig. 6. Effect of PPh@EDA recycling on the yield of 2-amino-tetrahydro-4*H*-chromenes and pyrans.

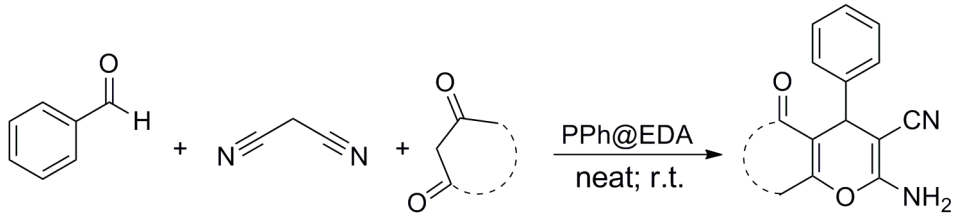

Scheme 1. Synthesis of a series of novel 2-amino-tetrahydro-4*H*-chromenes and pyrans.

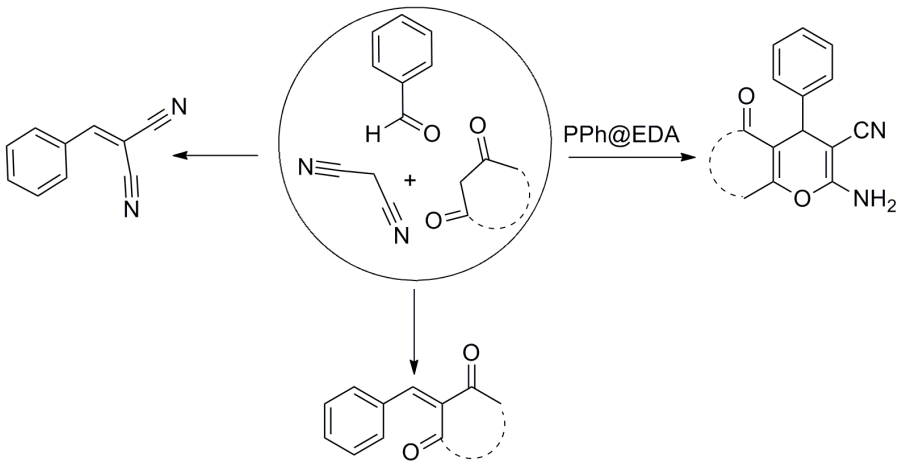

Scheme 2. Possible products formed during the one-pot synthesis of 2-amino-tetrahydro-4*H*-chromenes and pyrans.

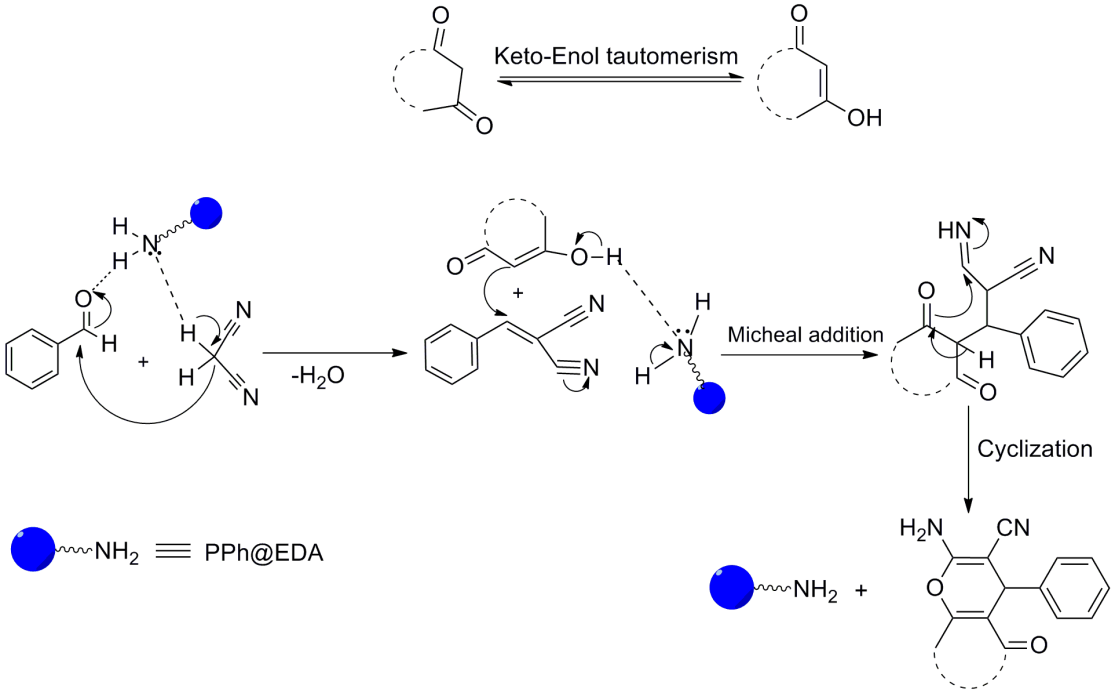

Scheme 3. A plausible mechanism for the formation of 2-amino-tetrahydro-4*H*-chromenes in presence of PPh@EDA.

Table 1. Effect of various catalysts on the synthesis of 2-amino-tetrahydro-4*H*-chromenes and pyrans.[a]

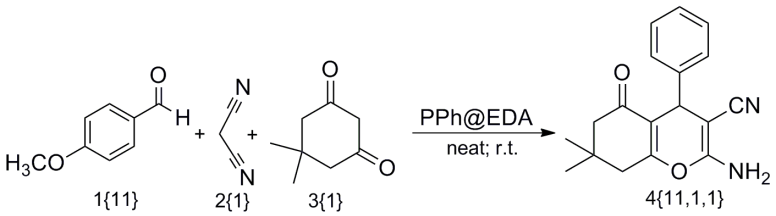

Entry	catalyst	Catalyst amount (%)	Time (h)	Yield (%)[b]	
				4	KC
1	Catalyst free	-	14	nr[c]	
2	$AlCl_3$	3 (mol %)	3	45	–
3	$FeCl_3$	3 (mol %)	4	50	–
4	$CuCl_2$	3 (mol %)	3.5	50	–
5	STA	3(mol %)	5	30	–
6	PSA	3 (mol %)	5	45	–
7	TSA	3 (mol %)	5	40	–
8	4-ethylmorpholine	3 (mol %)	1	80	20
9	4-ethylmorpholine	3 (mol %)	4	85	15
10	4-ethylmorpholine	3 (mol %)	8	90	10
11	Triethylamine	3 (mol %)	1	86	–
12	Tertiary butyl amine	3 (mol %)	0.5	88	–
13	TEMDA	3 (mol %)	0.5	90	–
14	Pyrrolidine	3 (mol%)	0.5	91	–
15	Piperidine	3 (mol%)	1	90	–
16	Diethylamine	3 (mol%)	0.5	91	–
17	Jeffamine (230)	3 (mol %)	0.5	92	–
18	Jeffamine (400)	3 (mol %)	0.7	90	–
19	Jeffamine (2000)	3 (mol %)	1	89	–
20	$MPEG_{2000}–NH_2$	3 (mol %)	1	86	–
21	PDMAEMA	3 (mol %)	1.5	85	–
22	Amberlite IRA–410	3 (mg)	2	86	–
23	$PPh@CH_2Br$	3 (mg)	6	45	–
24	PPh@EDA–0.2	0.6 (mol %)	3	80	–
25	PPh@EDA–0.4	1.2 (mol %)	2	83	–
26	PPh@EDA–0.6	1.8 (mol %)	1.5	80	–
27	PPh@EDA–0.6	3 (mol %)	1.4	82	–
28	PPh@EDA–0.6	3.6 (mol %)	1	87	–
29	PPh@EDA–0.6	4.8 (mol %)	1	91	–
30	PPh@EDA–0.6	6 (mol %)	1	95	–
31	PPh@EDA–0.6	7.8 (mol %)	1	95	–

[a]Experimental conditions: *p*-methoxybenzaldehyde = 1 mmol, malononitrile = 1 mmol, dimedone = 1 mmol, and catalyst = 10 mg at r.t. and neat condition.
[b]Isolated Yields.
[c]Noreaction.

Table 2. Effects of various solvents on the synthesis of compound **4**{11,1,1}.[a]

Entry	Solvent	Time (h)	Yield (%)
1	Solvent-free	1	95
2	EtOH	2	75
3	MeOH	3	79
4	IPA	2	83
5	THF	4	84
6	CH_2Cl_2	5	85
8	$CHCl_3$	6	85
9	1,4-Dioxane	4	80

[a]Experimental conditions: *p*-methoxybenzaldehyde = 1 mmol, malononitrile = 1 mmol, diimidone = 1 mmol, and catalyst = 10 mg at r.t.

Table 3. Substrate scope of the reaction.[a]

Entry	Product	Yield (%)[b]	Melting Point (°C)	
			Found	Reported
1	4{*1*,*1*,*1*}	92	224–225	225–226[33]
2	4{*2*,*1*,*1*}	90	214–216	216–217[33]
3	4{*3*,*1*,*1*}	91	151–153	150–152[38]
4	4{*4*,*1*,*1*}	92	228–230	229–230[33]
5	4{*5*,*1*,*1*}	94	204–206	206–208[36]
6	4{*6*,*1*,*1*}	89	203–205	202–204[38]
7	4{*7*,*1*,*1*}	91	178–180	–
8	4{*8*,*1*,*1*}	87	220–222	221–222[36]
9	4{*9*,*1*,*1*}	89	186–188	183–185[36]
10	4{*10*,*1*,*1*}	90	201–203	200–201[33]
11	4{*11*,*1*,*1*}	95	202–204	200–202[438]
12	4{*12*,*1*,*1*}	93	205–207	–
13	4{*13*,*1*,*1*}	95	209–210	208–210[36]
14	4{*14*,*1*,*1*}	94	206–209	–
15	4{*15*,*1*,*1*}	89	210–212	210–211[38]
16	4{*16*,*1*,*1*}	92	210–212	211–212[33]
17	4{*17*,*1*,*1*}	95	196–198	199–201[38]
18	4{*18*,*1*,*1*}	92	224–227	226–227[33]
19	4{*19*,*1*,*1*}	80	155–157	155–157[36]
20	4{*20*,*1*,*1*}	81	156–159	–
21	4{*1*,*1*,*2*}	90	232–234	232
22	4{*2*,*1*,*2*}	87	210–212	211–212
23	4{*9*,*1*,*2*}	93	236–238	237–239[38]
24	4{*11*,*1*,*2*}	95	196–198	197–199[38]
25	4{*16*,*1*,*2*}	93	232–234	232–233[36]
26	4{*1*,*1*,*3*}	92	160–162	160–162[46]
27	4{*2*,*1*,*3*}	90	148–150	148–150[46]
28	4{*3*,*1*,*3*}	91	138–140	138–140[46]
29	4{*4*,*1*,*3*}	94	140–142	140–142[46]
30	*4{5,1,3}*	95	134–136	134–136[46]
31	4{*9*,*1*,*3*}	93	150–152	150–152[36]
32	4{*1*,*1*,*4*}	91	190–192	192[36]
33	4{*1*,*1*,*5*}	92	170–172	–
34	4{*2*,*1*,*5*}	89	160–163	–
35	4{*3*,*1*,*5*}	90	158–160	–
36	4{*5*,*1*,*5*}	93	201–203	–
37	4{*10*,*1*,*5*}	92	165–168	–
38	4{*11*,*1*,*5*}	95	198–200	–
39	4{*14*,*1*,*5*}	94	168–170	–
40	4{*15*,*1*,*5*}	91	160–163	–
41	4{*16*,*1*,*5*}	95	175–177	–

42	4{*1,1,2*}	88	154–156	155–157[33]
43	4{2*1,1,1*}	–	–	–[c]

[a]Experimental conditions: *p*-methoxybenzaldehyde = 1 mmol, malononitrile = 1mmol, dimedone = 1 mmol, and catalyst = 10 mg at r.t. and neatcondition.

[b]Isolated yields.

[c]No reaction.

Table 4. Comparison of nonporous amines used for the synthesis of 2-amino-4*H*-chromenes and pyrans.

Compound	Catalyst (mole %)	Solvent	Time (h)	Yield (%)	Ref
4{11,1,1}	MCM–41–NH_2 (10)	H_2O	0.5	89	49
4{11,1,1}	MOF–NH_2 (6)	EtOH	4	92	50
4{11,1,1}	β-CD–NH_2 (5)	H_2O	3	91	51
4{11,1,4}	Chitosan (25)	H_2O	1.5	89	52
4{11,1,1}	PPh@EDA (10 mg)	Neat	1	95	This work[a]

[a]Experimental conditions: *p*-methoxy benzaldehyde = 1 mmol, malononitrile = 1 mmol, diimidone = 1 mmol, and catalyst = 10 mg at r.t. and neat condition.